

The Thermal Conductivity Reduction in HgTe/CdTe Superlattices

W. E. Bies and H. Ehrenreich

*Physics Department and Division of Engineering and Applied Sciences,
Harvard University, Cambridge, Massachusetts 02138*

E. Runge

*AG Halbleitertechnik, Inst. Physik,
Humboldt-Universität zu Berlin
Hausvogteiplatz 5-7, 10117 Berlin, Germany*

(Dated: December 2, 2001)

The techniques used previously to calculate the three-fold thermal conductivity reduction due to phonon dispersion in GaAs/AlAs superlattices (SLs) are applied to HgTe/CdTe SLs. The reduction factor is approximately the same, indicating that this SL may be applicable both as a photodetector and a thermoelectric cooler.

I. INTRODUCTION

Hg_xCd_{1-x}Te alloys are among the key materials used for cooled infra-red detectors. Materials structures involving these constituents in both alloy and superlattice (SL) forms that would be useful for both optical detection and thermoelectric cooling to a reasonably low temperature are an attractive possibility. Some semiconducting superlattices (SLs) are known to exhibit an order-of-magnitude reduction in the lattice thermal conductivities^{1,2,3,4,5,6,7,8,9,10}. For example, Capinski *et al* have experimentally shown GaAs/AlAs SLs to have a ten-fold smaller lattice thermal conductivity than the bulk alloys having the same composition^{11,12}. This result implies that the thermoelectric figure of merit ZT would be increased by an appreciable factor. We show theoretically that the same appears to be true for HgTe/CdTe SLs. Cooling of integrated room temperature devices to 200-250 K thus becomes a possibility for applications requiring no external coolant provided these temperatures are adequate. Since the devices would be fabricated of the same material constituents, manufacturing costs might be substantially reduced.

We have previously investigated GaAs/AlAs theoretically¹³ using Kunc's model for the lattice spectrum^{14,15} generalized to SLs¹⁶. Details are given in Ref. 13. This rigid-ion model considers next-nearest neighbor short-range forces together with the long-range Coulomb force. We found a factor-of-three reduction in the lattice thermal conductivity along the growth direction due to SL induced modifications of the phonon spectrum. The remainder of the overall ten-fold reduction is presumably associated with phonon scattering at the interfaces^{13,17,18} which is not considered in the present work. The thermal conductivity reduction in question here can be interpreted as resulting from zone folding in the SL relative to bulk. The new gaps introduced at the zone face result in band flattening and thus lower phonon velocities, which in turn reduce the thermal conduction. These effects are illustrated in Fig. 1 and Fig. 4 of Ref. 13. The corresponding figures in this paper will be seen to exhibit very similar effects

in HgTe/CdTe SLs. For reasons to be discussed, these results lead us to expect similar behavior in any SL having the same structure and similar mass and force constant differences between layers. Due to residual "impedance mismatches" at the interfaces, the Kunc model leads to decaying TA and LA modes along some intervals and directions in q -space. (This is not the case for GaAs/AlAs SLs.) We resolve this problem by use of a variety of physically motivated modifications, which are critically examined in the next section. The same three-fold reduction previously calculated for GaAs/AlAs is obtained. Moreover the result is shown to be robust with respect to the types of physically reasonable approximations made. Our discussion emphasizes that a reasonable phonon spectrum is obtained if one of the force constants, obtained from neutron diffraction experiments for HgTe and CdTe respectively, is modified by a small amount. Unfortunately there are no corresponding neutron data for the SL that might lead to better experimental input for determining the Kunc force constants.

II. THE KUNC MODEL FOR HgTe/CdTe SLs

The Kunc rigid-ion model^{14,15} has been successfully applied to compounds with zinc-blende structure. In each bulk compound, ten parameters describe the force constants between nearest and next-nearest neighbors and one parameter the effective charge. In the absence of experimental data for HgTe/CdTe SLs there are no directly determinable parameters with which to fit the phonon spectrum. Note that even for bulk HgTe the fit to the neutron-diffraction data along the [111] direction does not reproduce the optical branches very well¹⁹. Thus, we use the parameter fits to bulk HgTe and CdTe determined by Talwar and Vandevyver¹⁹ and construct the SL dynamical matrix from these. There are thus 22 parameters needed for the SL, in addition to the atomic masses and lattice spacing. The bulk parameters are used within each layer. At the interface we average the force constants from the two sides. The Madelung sum is cal-

culated using the Ewald transformation adapted to the SL. We refer to Ref. 13 for the details. The output of the Kunc model is the phonon dispersion $\omega_{\mathbf{q}}^{(\alpha)}$ for the α -th branch as a function of wavevector \mathbf{q} in the SL Brillouin zone. The lattice thermal conductivity may then be computed from the phonon Boltzmann equation in the relaxation-time approximation:

$$(\kappa_{\ell})_{ij} = \int \frac{d^3q}{(2\pi)^3} \left[\sum_{\alpha} \hbar \omega_{\mathbf{q}}^{(\alpha)} \frac{\partial \omega_{\mathbf{q}}^{(\alpha)}}{\partial q_i} \frac{\partial \omega_{\mathbf{q}}^{(\alpha)}}{\partial q_j} \frac{dn(\omega_{\mathbf{q}}^{(\alpha)})}{dT} \right] \times \tau_{\text{ph}}(\omega_{\mathbf{q}}^{(\alpha)}, T), \quad (1)$$

where $n(\omega_{\mathbf{q}}^{(\alpha)})$ is the distribution function of phonons and $\tau_{\text{ph}}(\omega_{\mathbf{q}}^{(\alpha)}, T)$ is the lifetime, taken to be a constant τ .

The dynamical matrix for the HgTe/CdTe SL so constructed, though Hermitian, has negative eigenvalues, i.e., yields imaginary phonon frequencies, for the three acoustic branches in a cylindrical region of the Brillouin zone around the [001] axis that occupies about 6% of the zone by volume. The problem of imaginary frequencies in models of HgTe/CdTe SLs has been investigated by Rajput and Browne.²⁰ They attribute the problem to an inadequate modelling of the interface, in their simple force model based on the Keating potential. They find that in their model the imaginary frequencies can be removed by treating the two materials as continuum media with differing dielectric constants. However, this prescription fails to remove the imaginary frequencies using the Kunc model. As we shall see below, the imaginary frequencies in the Kunc model are more likely to arise from the force constants than from the Coulomb interaction.

In order to gain an idea of what is causing the imaginary frequencies, we looked at the dependence of the gap at the zone edge, $\Delta\omega$, on the Kunc parameters. We found the strongest dependence for the diagonal terms in the force constant matrices; the effect of the off-diagonal terms was weaker by a factor of ten or more. This finding motivated us to consider the variation of the parameters necessary to remove imaginary frequencies. For example, an interpolation of all parameters (20 force constants, 2 effective charges, 3 atomic masses and the lattice spacing) linearly between their values for a HgTe/CdTe SL ($x = 0$) and those for a GaAs/AlAs ($x = 1$), which has real frequencies only, shows that all of the imaginary frequencies disappear when x approaches 0.035. This suggests that we associate the imaginary frequencies with an impedance mismatch between the HgTe and CdTe layers which can be removed by variation of appropriate force constants or the introduction of additional ones provided by a more sophisticated model. Thus, if we hold the parameters fixed at their HgTe/CdTe values and vary the parameters individually, we find that small ($< 10\%$) changes in A_{HgTe} and A_{CdTe} alone are sufficient to yield real frequencies throughout the SL Brillouin zone. Here, A is the nearest-neighbor coupling between Hg and Te respectively Cd and Te. Apparently the problem does not exist in GaAs/AlAs SLs because the A pa-

rameters are so closely matched: $A_{\text{GaAs}} = -40.77$ N/m and $A_{\text{AlAs}} = -40.83$ N/m.

We now describe our approaches for removing the imaginary frequencies. The only correct way to solve the problem is to generalize the already complicated Kunc model. However, the Kunc-model description of the bulk phonon dispersion is satisfactory. Changing the bulk model does not necessarily imply that the SL results will be improved because the interfaces are neglected. Instead, we construct physical models, for example, determining values of A that eliminate the imaginary frequencies. The reduction factor is always about 3 for the more realistic models. The robustness of the result gives us more confidence in its physical relevance than would deriving it from a generalized Kunc model with many new parameters.

The best model utilizes scaling, which maintains the acoustical and optical mode frequencies observed in bulk. The effect of changing A , aside from removing the imaginary frequencies, is to rescale all the phonon frequencies across the Brillouin zone. The scaling model is therefore constructed as follows: (1) A is replaced by A' ; in practice A' is selected so that the ratio of LA to TA sound velocities in the [001] direction will be that of bulk; this means $x = 0.2$ or A_{HgTe} is changed from -18.127 N/m to -22.7 N/m and A_{CdTe} from -19.97 N/m to -24.1 N/m. This gives sound velocities about 10% too high and increases the frequencies of the optical branches by 10%. (2) In order to compensate for this increase, all phonon frequencies are rescaled by a common factor, $\omega \rightarrow \lambda\omega$, with $\lambda = 0.927$, assuming λ to be constant. The scaling model has the advantage of staying within the Kunc-model framework, while removing the imaginary frequencies in a consistent way.

Another model is based on averaging the force constants (both nearest neighbor and next-nearest neighbor) at the interface. This approach serves to equalize the force experienced in each direction by the interfacial Te ion. This approach fails, however, to remove the imaginary frequencies. The fraction of the Brillouin zone covered by imaginary frequencies changes by less than 1%.

The problem can be addressed most simply by setting the frequencies of the imaginary branches equal to zero. We find a thermal conductivity reduction by a factor of 3.0, very close to that found for GaAs/AlAs. Since only three of the eighteen folded-back acoustic branches are set to zero over a small part of the zone, the end result should be close to the true value, which represents a lower bound to the reduction factor. For comparison, we find that setting the lowest three branches to zero in GaAs/AlAs gives a reduction by a factor of 2.9, versus 2.8 in the correct calculation. Thus we can expect that the actual value in HgTe/CdTe will be close to 3.

Another approach involves a linear interpolation from the origin to the point of tangency with the acoustic branches where they are real. This gives a reduction factor of 2.9. The treatment of the acoustic branches however is unrealistic because the interpolated sound ve-

locities are too low, only about 50% of the bulk value (average of HgTe and CdTe) in the [001] direction.

The simplest model is based on the virtual crystal approximation, in which the force constants are replaced with their averages between the two layers, while the masses and effective charges are kept at their respective values for the two layers. This ensures that the frequencies are real, because of the absence of interfaces. However, it does not properly account for the thermal conductivity reduction (giving only a factor of 1.3), because the band gaps at the zone edge, which reduce the phonon velocity, are considerably smaller than they should be. These results indicate that it is the force constants and not the Coulomb interaction that are responsible for the imaginary frequencies in the SL Kunc model.

III. RESULTS

We consider a (HgTe)₃/(CdTe)₃ SL. The dispersion relation along the ΓX and ΓZ directions was generated numerically using the scaling model as described in Sec. II and is shown in Fig. 1. The SL unit cell contains three unit cells each of HgTe and CdTe, arranged along the growth axis. Thus, the edge of the SL Brillouin zone is one-sixth as far from the center along the ΓZ axis as it is in the in-plane ΓX and ΓY directions. Each of the six branches in bulk is folded back six times in the ΓZ direction, yielding 36 branches in the SL. This effect is most easily seen for the acoustic modes along ΓZ . The results are qualitatively similar to those obtained for (GaAs)₃/(AlAs)₃ in Ref. 13. The HgTe and CdTe optical modes are not as well separated as the GaAs and AlAs optical modes are in GaAs/AlAs, and we see that the lowest HgTe optical modes overlap with the highest acoustic modes along ΓX . Nevertheless, the optical modes are nearly flat in the ΓZ direction.

As can be seen in Fig. 1, the physical effects of band flattening, relative to bulk, are present. We therefore expect, by Eq. (1), a reduction in the thermal conductivity along the growth axis. In fact, with our data, Eq. (1) yields a reduction factor in κ/τ of 3.0 (in the scaling model). This factor reflects phonon-dispersion effects only. As discussed in Ref. 13, one may expect a further reduction in thermal conductivity if the lifetime τ itself is lowered in the SL compared to bulk due primarily to interface scattering. But there is not sufficient data on HgTe/CdTe SLs for us to discuss the lifetime quantitatively.

A simple physical picture of the thermal conductivity reduction due to phonon dispersion effects is obtained by looking at the transport quantity $q_x \sum_{\alpha} (dn(\omega_{\mathbf{q}}^{(\alpha)})/dT) \omega_{\mathbf{q}}^{(\alpha)} (v_{\mathbf{q},z}^{(\alpha)})^2$ in \mathbf{q} space. This is the quantity in square brackets in Eq. (1). Since the dispersion relation is rotationally symmetric in the (q_x, q_y) plane to good approximation we perform an annular integration, yielding the factor q_x equal to the annular radius and leaving an integral in Eq. (1) depending only on q_x

and q_z . The resulting quantity is plotted in Figs. 2(a), 2(b) and 2(c) for the SL and for bulk HgTe as a function of q_z for three values of q_x . The SL transport quantity is seen to be localized, i.e., it tends to zero at the band edges $q_z = 0$ and $q_z = \pi/d$. The reduction in the SL transport quantity near the zone edges is related to miniband formation (the flattening of ω versus q_z seen in Fig. 1). To gain physical insight, we replace the SL transport quantity in Figs. 2(a), (b) and (c) by rectangles of equal area and plot these in Fig. 2(d), which summarizes the dependence of the transport quantity on q_x . The shading indicates the weight of each equivalent rectangle within the range $(q_x, q_x + \Delta q_x)$. In bulk the equivalent rectangles extend all the way to the zone edges because there is no localization due to band flattening. In Fig. 2(d) we see that the densities tend to zero as q_x goes to zero and that the density in bulk increases for large q_x , again due to the q_x prefactor. Surprisingly, the density in the SL falls off fast enough as q_x increases to overcome the q_x factor. This should be compared with the results for GaAs/AlAs SLs of Ref. 13. The qualitative difference between HgTe/CdTe and GaAs/AlAs SLs is not apparent from their dispersion relations. Integrating the density in Fig. 2 gives an estimated reduction factor of 2.4, which is to be compared with 3.0 in the exact calculation. The difference is due to the fact that the estimate does not properly treat the region of the Brillouin zone with radius greater than $\sqrt{2}\pi/a_0$ and therefore underestimates the reduction factor.

Our results predict a reduction factor in thermal conductivity for HgTe/CdTe SLs comparable in size to those already observed for GaAs/AlAs SLs. The minimum cold temperature achievable for a 30Å Hg_{0.75}Cd_{0.25}Te/30Å Hg_{0.7}Cd_{0.3}Te SL is about 180 K, compared to 240 K for conventional Bi₂Te₃. This result suggests that it is reasonable to use HgCdTe for thermoelectric cooling applications in infra-red detectors.

IV. ACKNOWLEDGMENTS

The authors wish to thank C.H. Grein for helpful discussions. This work was supported by DARPA through ARL Contract No. DAAD17-00-C-0134.

- ¹ L. D. Hicks and M. S. Dresselhaus, *Phys. Rev. B* **47**, 12727 (1993).
- ² P. J. Lin-Chung and T. L. Reinecke, *Phys. Rev. B* **51**, 13244 (1995).
- ³ D. A. Broido and T. L. Reinecke, *Phys. Rev. B* **51**, 13797 (1995).
- ⁴ D. A. Broido and T. L. Reinecke, *Appl. Phys. Lett.* **67**, 1170 (1995).
- ⁵ P. Hyldgaard and G. D. Mahan, *Phys. Rev. B* **56**, 10754 (1997).
- ⁶ S.-I. Tamura, Y. Tanaka and H. J. Maris, *Phys. Rev. B* **60**, 2627 (1999).
- ⁷ G. Chen and M. Neagu, *Appl. Phys. Lett.* **71**, 2761 (1997).
- ⁸ G. D. Mahan and L. M. Woods, *Phys. Rev. Lett.* **80**, 4016 (1998).
- ⁹ G. D. Mahan, J. O. Sofo and M. Bartkowiak, *J. Appl. Phys.* **83**, 4683 (1998).
- ¹⁰ R. J. Radtke, H. Ehrenreich and C. H. Grein, *J. Appl. Phys.* **86**, 3195 (1999).
- ¹¹ W. S. Capinski and H. J. Maris, *Physica B* **219**, 299 (1996).
- ¹² W. S. Capinski, H. J. Maris, T. Ruf, M. Cardona, K. Ploog and D. S. Katzer, *Phys. Rev. B* **59**, 8105 (1999).
- ¹³ W. E. Bies, R. J. Radtke and H. Ehrenreich, *J. Appl. Phys.* **88**, 1498 (2000). This paper contains all the basic references.
- ¹⁴ K. Kunc, *Ann. Phys. (Paris)* **8**, 319 (1973-1974).
- ¹⁵ K. Kunc, M. Balkanski and M. A. Nusimovici, *Phys. Rev. B* **12**, 4346 (1975).
- ¹⁶ S.-F. Ren, H. Chu and Y.-C. Chang, *Phys. Rev. B* **37**, 8899 (1988).
- ¹⁷ G. Chen, *J. Heat Transfer* **119**, 220 (1996).
- ¹⁸ G. Chen, *Phys. Rev. B* **57**, 14958 (1998).
- ¹⁹ D. N. Talwar and M. Vandevyver, *J. Appl. Phys.* **56**, 1601 (1984).
- ²⁰ B. D. Rajput and D. A. Browne, *J. Phys.: Cond. Matter* **10**, 3177 (1998).

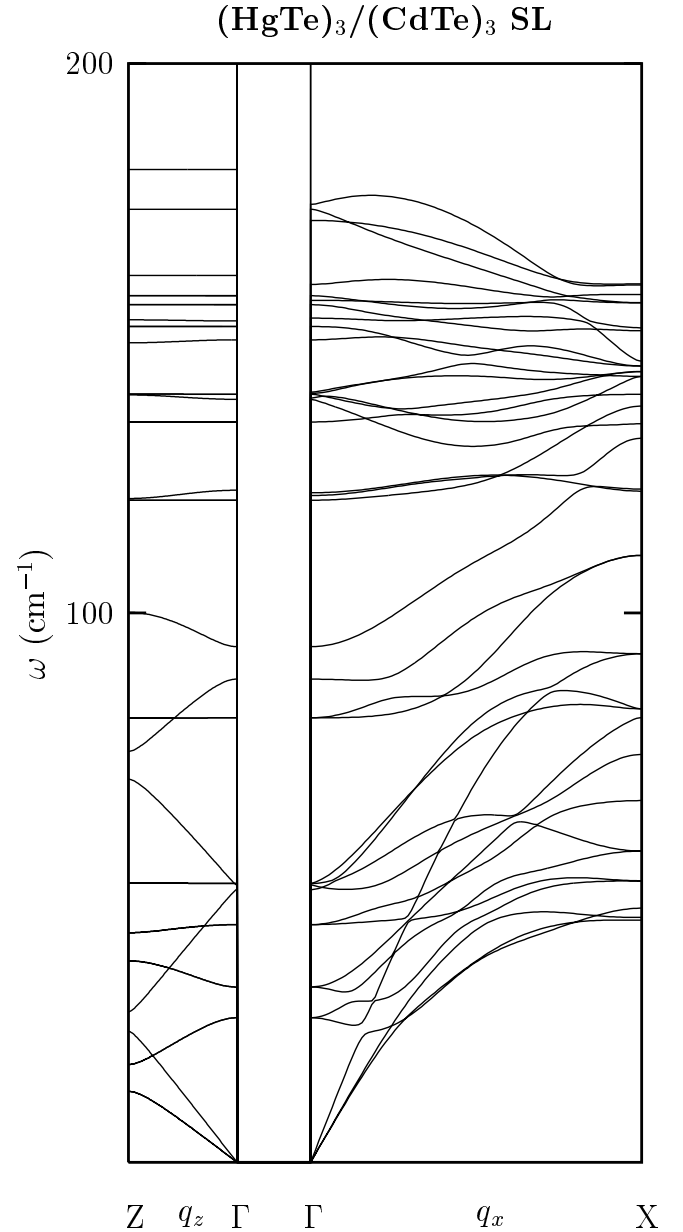


FIG. 1: (HgTe)₃/(CdTe)₃ superlattice dispersion relation along the $\Gamma X=(2\pi/a_0, 0, 0)$ and $\Gamma Z=(0, 0, \pi/3a_0)$ directions, where $a_0 = 6.48 \text{ \AA}$ is the conventional unit cell size of bulk HgTe.

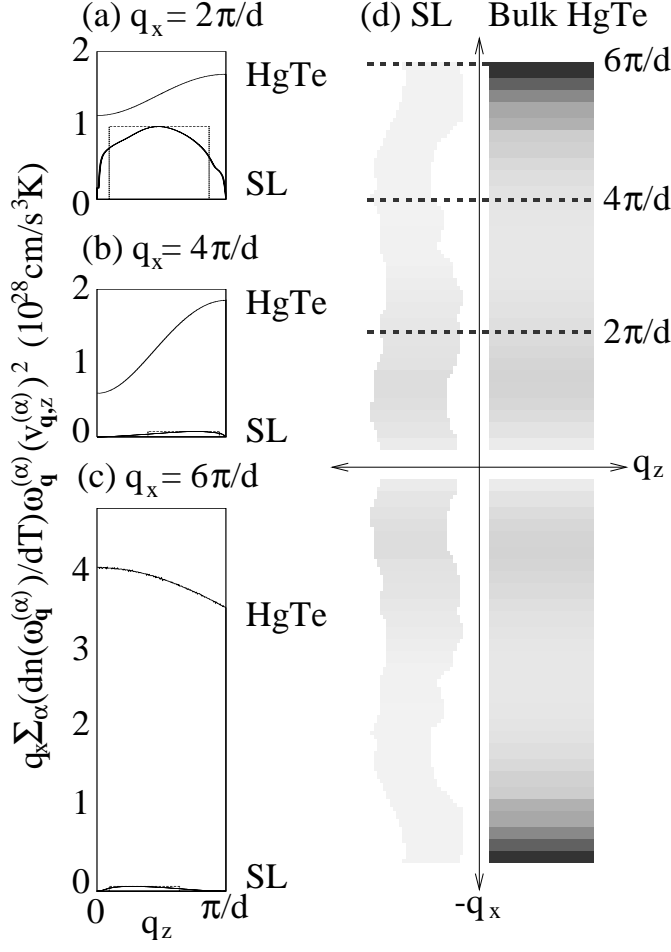


FIG. 2: (a),(b),(c) The transport quantity $q_x \sum_{\alpha} (dn/dT) \omega_{\mathbf{q}}^{(\alpha)} (v_{\mathbf{q},z}^{(\alpha)})^2$ for $0 \leq q_z \leq \pi/d$ at fixed q_x for (a) $q_x = 2\pi/d$, (b) $q_x = 4\pi/d$ and (c) $q_x = 6\pi/d$. The bulk HgTe and the $(\text{HgTe})_3/(\text{CdTe})_3$ SL curves are labelled on the right of figures (a), (b), and (c). Note the smallness of the SL curves in (b) and (c). (d) Density plot in the (q_x, q_z) plane whose shading indicates the weight of each increment in Δq_x along q_x to the value of the transport quantity for the $(\text{HgTe})_3/(\text{CdTe})_3$ SL and bulk HgTe respectively.